ACCELERATED PD-AGING OF SOLID INSULATING MATERIALS UNDER HIGH FREQUENCY HIGH VOLTAGE STRESS

Michael Kempf, M. Sc.*, Prof. Dr. sc. Myriam Koch

High Voltage Laboratories, TU Darmstadt, Darmstadt, Germany

Due to an increased integration of power electronic components in power grids and the continuous development of power semiconductors, insulation materials are exposed not only to high electric fields but simultaneously to strongly increased frequencies. This combination poses greater stress on most insulating materials compared to conventional operation. Thereby, both, their short- and long-term behavior can be negatively affected. Due to higher dielectric losses and the associated heat generated leading to accelerated aging of the material. The aim of this study is to investigate the aging behavior of solid insulating materials under the presence of partial discharges at high frequency test voltages. These results are compared with aging under 50 Hz stress. For this purpose, various long-term studies are conducted on epoxy resin test samples at different frequencies and voltage waveforms. As test voltages, both, sinusoidal high frequency high voltages (HFHV) and so-called mixed-frequency high voltages (MXF-HV) are used. The high frequencies range from 20 kHz to 2.5 MHz. As indicators of the test samples aging state the change of the dielectric parameters as well as the breakdown field strengths of the test samples are examined. In addition, the reduction in lifetime due to different partial discharge aging stresses is evaluated.

1. Motivation

The requirements for solid insulating materials in the area of energy technology are steadily increasing. This is, for example, due to the growing integration of power electronic components in power grids and increasing switching frequencies due to the availability of wide-bandgap semiconductors [1-2]. Thus, insulating materials are increasingly exposed to a combination of high electric fields and simultaneously high frequencies [3-4]. This can affect, for instance, insulating materials from the area of high voltage engineering (e.g. cable insulations, cable joints, epoxy resin mica insulations in rotating machines, surge arresters), as well as the insulation in power semiconductors and converters. The described stress can impact the short- as well as the long-term behavior of insulating materials in a negative way. The existing knowledge about the dielectric behavior of the materials in a frequency range of up to several megahertz is entirely inadequate to make systematic statements about their withstand capability, insulation failure, or aging [4]. In particular, the frequency-, field strength-, and temperature-dependent dielectric loss mechanisms as well as accelerated aging behavior, need to be further investigated.

2. Experimental setups

2.1. Test setup for generating HFHV

For the generation of high frequency high voltage (HFHV) with frequencies up to the MHz range, conventional high voltage transformers

with iron or ferrite cores cannot be used. A suitable alternative for generating HFHV is the use of series resonant circuits, which are excited by an inverter. The simplified equivalent circuit diagram of such an experimental setup is shown in Figure 1.

Fundamentally the DC voltage $U_{\rm DC}$ is converted into an alternating square wave voltage $U_{\rm sq}$ using a frequency-variable inverter. In this case, the switching frequency $f_{\rm res}$ of the inverter corresponds to the resonance frequency of the series resonant circuit. The resonant circuit consists of a variable air coil $L_{\rm res}$, a variable vacuum capacitor $C_{\rm res}$, and the capacitance of the test object $C_{\rm DUT}$. By exciting the resonant circuit with the resulting alternating voltage $U_{\rm sq}$, a sinusoidal high frequency high voltage $U_{\rm HFHV}$ with the frequency of the resonant circuit can be generated at the device under test (DUT). Since the quality factor of high frequency resonant circuits is high, only a comparatively low input DC

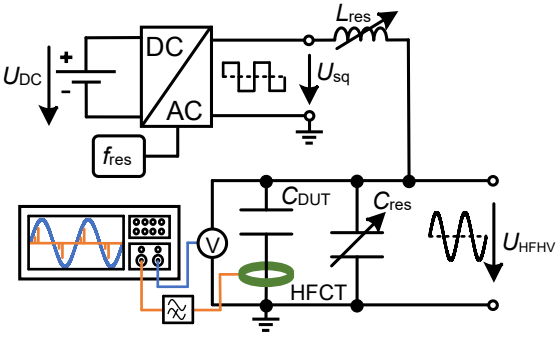


Figure 1: Concept for generating HFHV up to 5 MHz using a series resonant circuit

voltage U_{DC} is necessary to generate voltages in the range of several kilovolts.

For the detection of partial discharges, a broadband current transformer (HFCT) according to [5] is used, which is integrated into the ground path of the test specimen. The voltage is measured using a broadband high voltage probe with a low input capacitance (<3 pF).

2.2. Test setup for generating MXF-HV

For generating the mixed-frequency high voltage (MXF-HF), a 50 Hz voltage is superimposed with an HFHV with a frequency of 20 kHz. The amplitude of the HFHV is 20 % of the amplitude of the 50 Hz voltage. The simplified experimental setup used for this purpose is shown in Figure 2.

The HFHV is generated as described in Section 2.1. To protect the inverter from the low frequency high voltage, the resonant circuit is extended with a blocking capacitor C_B ($C_B \gg C_{res}$).

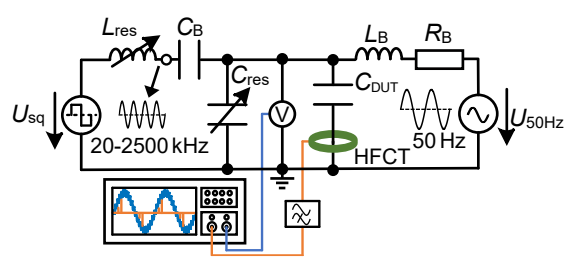


Figure 2: Concept for generating mixed-frequency voltages by superimposing a 50 Hz HV with high frequency high voltage

The 50 Hz voltage is generated using a standard high voltage transformer. To protect the transformer from the HFHV, it is connected to the resonant circuit via a high-ohmic resistor and a coil. At the resonance capacitor C_{res} the mixed-frequency high voltage can be tapped.

2.3. Electrode configuration

For a reproducible PD generation on the surface of the test samples a sphere-plate arrangement was used. All electrodes are made of stainless steel. A schematic cross-section of the arrangement, including a test sample, is shown in Figure 3. In this arrangement, the HV electrode (sphere), the test specimen ($\varepsilon_r \approx 3.5$), and the surrounding air ($\varepsilon_r \approx 1$), form a triple point (TP). Due to field displacement, the air in the vicinity of the triple point is stressed with an electric field strength approximately 3.5 times higher than the epoxy resin test sample. Due to the lower dielectric strength of air, partial discharges preferentially and reproducibly occur in the air region of the triple point. Depending on the applied voltage, the discharges spread radially on the surface of the test sample (Figure 3b and 3c).

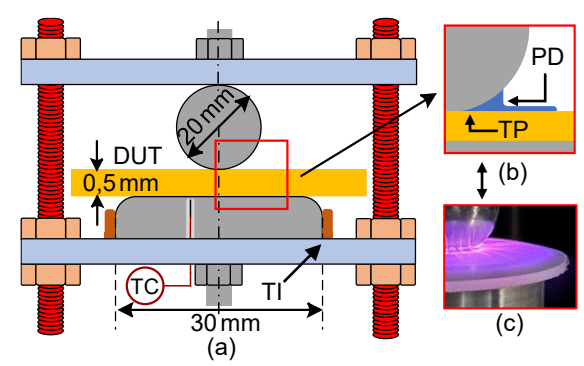


Figure 3: (a) Schematic cross-section of the electrode configuration and (b) a schematic representation as well as (c) a picture of the triple point and the propagating PD

As an additional factor influencing the material stress, the temperature of the test samples is measured indirectly using a thermocouple (TC) embedded in the ground electrode. To minimize heat dissipation from the ground electrode to the surrounding air, the electrode was covered in a thermal insulation (TI).

2.4. Test samples

As test samples an unmodified epoxy resin in shape of thin disks was used. The thickness of the test samples $t_{\rm DUT}$ is between 0.45 mm and 0.55 mm. The diameter is 45 mm. For each combination of frequency and test voltage level (Table 1), 10 test samples were used for the destructive and 15 test samples for the non-destructive aging tests. Before the measurements, the test samples were dried in a vacuum at 60 °C. Between the measurements the test samples were stored in a desiccator at room temperature.

3. Experimental procedures

The used voltage types as well as the respective frequency and voltage levels were identical for both approaches and can be found in Table 1. The inception voltage for each test sample was determined individually. Table 1 represents the values using the example of a test sample with a thickness of 0.51 mm. The absence of the higher

Table 1: Overview of the frequency and test voltage level combinations as well as exemplary PD inception voltages \hat{U}_i for t_{DUT} = 0.51 mm

Voltage type	Frequency	PD inception voltage \hat{U}_{i}	Test voltage $\hat{\mathcal{U}}_t$
Reference	50 Hz	2.52 kV	$\hat{U}_i \mid 1.5 \cdot \hat{U}_i \mid 2 \cdot \hat{U}_i$
MXF-HV	50 Hz + 20 kHz	2.52kV	$\hat{\mathcal{U}}_i \mid 1.5 \cdot \hat{\mathcal{U}}_i \mid 2 \cdot \hat{\mathcal{U}}_i$
HFHV	20 kHz	2.55 kV	$\hat{U}_i \mid 1.5 \cdot \hat{U}_i \mid 2 \cdot \hat{U}_i$
	40 kHz	2.57 kV	$\hat{U}_i \mid 1.5 \cdot \hat{U}_i \mid 2 \cdot \hat{U}_i$
	130 kHz	2.84 kV	$\hat{U}_{i} \mid 1.5 \cdot \hat{U}_{i}$
	2.5 MHz	3.13 kV	$\hat{m{U}}_{i}$

voltage levels at 130 kHz and 2.5 MHz is due to the fact that the test samples failed before reaching the respective voltage. The increase in the PD-inception voltage with increasing frequency can mainly be justified to the decrease in relative permittivity (Figure 6). As a result, the effect of field displacement is weakened, leading to less field strength being displaced in the air gap.

3.1. Destructive aging tests

The aim of the destructive aging tests is to determine the maximum duration until failure of the test samples, depending on the combination of frequency and voltage level chosen. For this purpose, the test samples were tested for different combinations of voltage and frequency (Table 1) under constant environmental conditions up to a maximum duration of 10 weeks. Based on these measurement series, the expected lifetime with the presence of PD can be determined, depending on the different stress scenarios. Furthermore, the maximum duration of stress for the non-destructive aging experiments can be derived.

3.2. Non-destructive aging tests

As a part of the non-destructive aging tests, the influence of PD-aging on the dielectric properties and on the breakdown field strength of the epoxy resin samples is investigated. The procedure is as follows:

- (a) Material characterization
- (b) PD-aging under HFHV/MXF-HF stress
- (c) Material characterization after the PD-aging
- (d) Short-term breakdown tests (aged samples)

In the first step (a), the samples are characterized in terms of their dielectric properties (DC volume conductivity, relative permittivity, and loss factor). The duration of the stress in step (b) depends on the determined time until failure of the test specimens from the destructive aging test. After the PD-aging in step (c), the test samples are again characterized in terms of their dielectric properties. As the last step (d), shortterm breakdown tests according to [6] are conducted with 50 Hz voltage. In this case also, a sphere-plate electrode arrangement was used. To prevent surface discharges, insulating oil is used as surrounding medium. Since the thickness of each test specimen is not exactly the same (cf. Section 2.4), the resulting breakdown voltages are related to a test specimen thickness of 0.5 mm according to [7], taking the volume/thickness effect into account.

4. Results

4.1. Destructive aging tests

The influence of the selected combinations of field strength and frequency for the measurement series under HFHV stress is shown in Figure 4. The measurement data are presented as box plots. These consist (for all following figures) of the median, the 25% and 75% quantile, as well as whiskers which represent the minimum and maximum values. Since no test sample failed during the measurement series with both, power frequency and MXF-HV these measurement series are not shown in Figure 4.

For the measurement series using HFHV stress, it can be observed that the average lifetime of the test samples decreases significantly with both increasing frequency and increasing field strength. For instance, doubling the frequency from 20 kHz to 40 kHz results in a reduction of the average lifetime by approximately 60%. With a further increase of the frequency up to 2.5 MHz, the average lifetime decreases by 99.3% to approximately 30 seconds. A comparable significant reduction in lifetime is achieved by increasing the applied voltage. For example, at a test frequency of 40 kHz an increase of the applied voltage from $1 \cdot \hat{U}_i$ to $2 \cdot \hat{U}_i$ results in a lifetime reduction by approximately 93%.

Furthermore, the influence of an increased voltage appears to intensify with rising frequency. Comparing the results at 130 kHz (compared to 20 kHz and 40 kHz) an increase of the voltage from $1 \cdot \hat{U}_i$ to $1.5 \cdot \hat{U}_i$ was sufficient to reduce the average lifetime of the test samples by approximately 97 %. Due to this effect, the test specimens failed before reaching $2 \cdot \hat{U}_i$ at 130 kHz as well as $1.5 \cdot \hat{U}_i$ at 2.5 MHz, respectively.

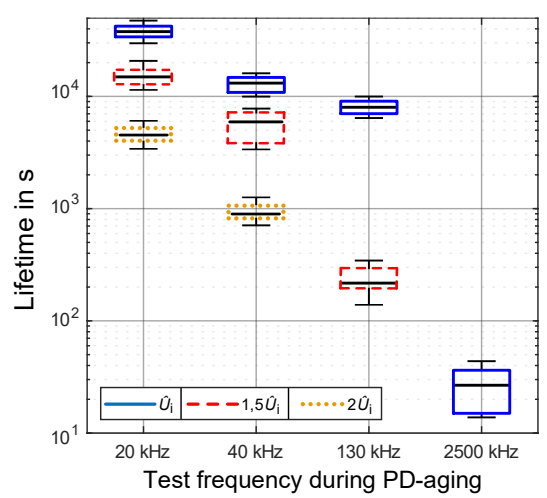


Figure 4: Impact of PD-aging on the lifetime of material test samples for the indicated combinations of field strength and frequency

4.2. Non-destructive aging tests

4.2.1. Impact on the dielectric parameters

The partial discharge aging has led to a change of the dielectric parameters in most scenarios. For a better overview, scenarios where the dielectric characteristics have not changed significantly are neglected in the following graphics.

The change in DC volume conductivity of the samples is summarized in Figure 5. In the measurement series using HFHV, the changes in conductivity can be detected already at $1 \cdot \hat{U}_{i}$. For the test frequencies of 20 kHz and 40 kHz a slight increase can be observed and for a frequency of 130 kHz, an average increase of approximately 52% is shown. Additionally, an increase in voltage reveals a stronger aging effect in form of an increasing conductivity. Thus, the conductivity increased by over 200 % for the HFHV measurement series at a voltage of $2 \cdot \hat{U}_i$. In comparison, only a slight increase can be detected for the 50 Hz and MXF-HV measurement series, even for a test voltage level of $2 \cdot \hat{U}_i$. The HFHV measurement series with a frequency of 2.5 MHz deviates from the usual observations. Despite the higher frequency a less aging effect as for the other HFHV measurement series was observed.

The partial discharge aging has had less overall impact on the relative permittivity (Figure 6). The relative permittivity is plotted on the x-axis over a frequency range from 0.1 Hz to 5 kHz. This frequency range represents the frequencies at which the relative permittivity was determined after the PD-aging. Only the most critical scenarios have, on average, resulted in a minimal increase in relative permittivity. The maximum increase of around 3% occurred at 40 kHz and $2\cdot\hat{U}_i$. Apart from the three stress scenarios listed separately in Figure 6, no significant deviation in permittivity could be identified in the HFHV scenarios.

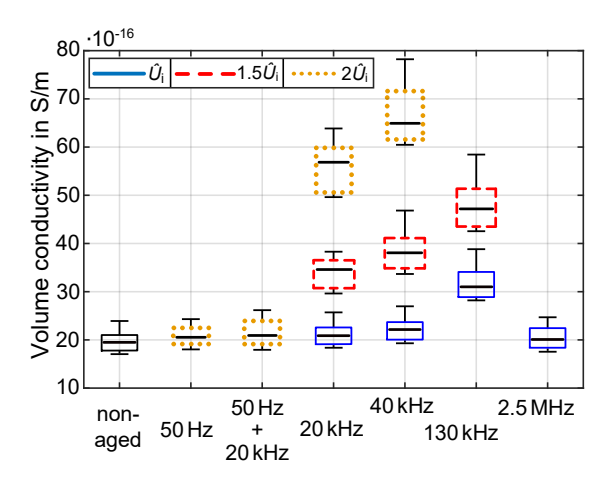


Figure 5: Change in DC volume conductivity due to PD-aging

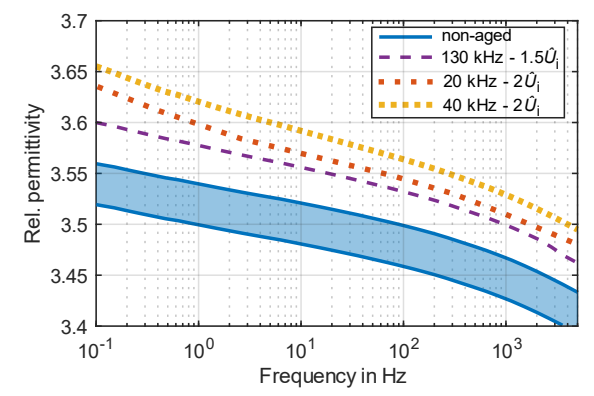


Figure 6: Change in relative permittivity at various combinations of field strength and frequency

In Figure 7, the loss factor is shown over a frequency range from 0.1 Hz to 5 kHz. As for the relative permittivity, the frequencies on the x-axis represent the frequency range over which the loss factor was measured after aging, rather than the frequencies at which the material has been aged. Due to its strong dependence on conductivity, PD-aging has a comparable impact on the loss factor as it does on conductivity. At a test voltage level of $1 \cdot \hat{U}_i$, only a slight increase can be detected for test frequencies of 20 kHz and 40 kHz. On the other hand, there is a significant increase in the loss factor at a test frequency of 130 kHz. In principle, the increase in the loss factor in these measurement series appears to be more pronounced at lower frequencies ($\leq 10 \,\text{Hz}$)

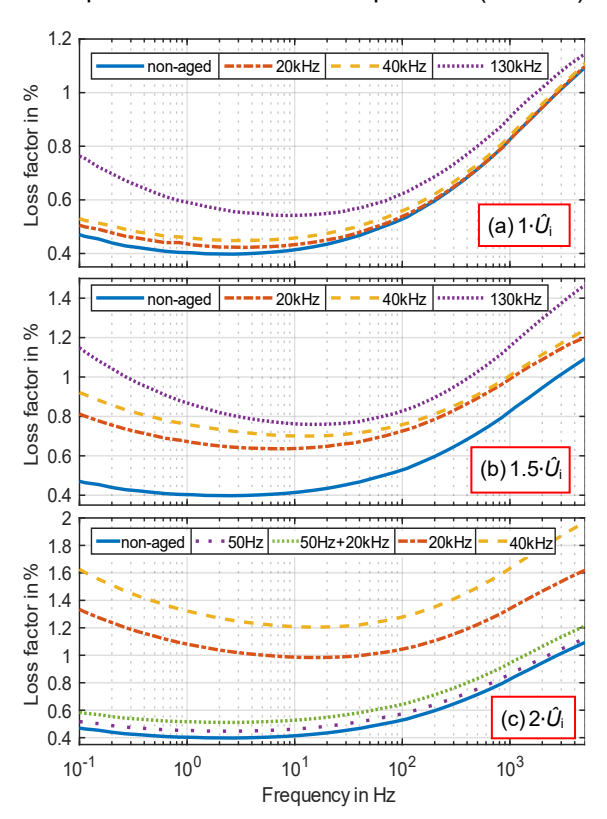


Figure 7: Change in loss factor due to PD-aging

than at higher frequencies (Figure 7a). By increasing the test voltage to $1.5 \cdot \hat{U}_i$ the aging effect intensifies. Especially at a test frequency of 130 kHz, an increase in the loss factor at higher measurement frequencies (>100 Hz) becomes noticeable (Figure 7b). As for the other two dielectric parameters, the maximum change is reached at a test voltage level of $2 \cdot \hat{U}_i$ and a frequency of 40 kHz (Figure 7c).

4.2.2. Impact on the breakdown field strength

The results of the breakdown investigations are summarized in Figure 8. In addition to the breakdown field strengths, exemplary images of a test sample before the breakdown tests are shown for each combination of frequency and field strength. These images provide insights into both, the size of the degraded area and the degree of degradation resulting from various partial discharge stresses.

In almost all aging scenarios, the breakdown field strength has decreased compared to the non-aged test samples. As for the dielectric parameters, the PD-aging affects the material samples more critically with both, an increase in aging field strength and an increase in frequency. The maximum reduction in breakdown field strength is approximately 35%, occurring at a frequency of 130 kHz for both, $1 \cdot \hat{U}_i$ and $1.5 \cdot \hat{U}_i$. This result differs from the results of Section 4.2.1. Here, for all three dielectric parameters, the test series with a test voltage level of $2 \cdot \hat{U}_i$ had the most impact. Another notable observation is evident in the measurements with MXF-HV at $2 \cdot \hat{U}_i$. In these measurement series, only a slight aging effect could be observed in terms of the change in the dielectric parameters. In terms of breakdown field strength, this measurement series demonstrates a comparable decrease to the other measurement series. The minimum reduction in breakdown field strength

could be detected for a frequency of 2.5 MHz and a test voltage level of $1 \cdot \hat{U}_{i}$.

5. Discussion

The results clearly imply that the PD stress on the test samples has increased with additional high frequency components. This is indicated by reduced lifetimes as well as a decrease in the insulation capability of the material within the electrode arrangement used. Furthermore, a change in the dielectric parameters can be observed. In particular, the increase in conductivity and the associated increase in loss factor are also indications of advanced aging. On the other hand, PD-aging had a slight to no effect on the relative permittivity.

These observations can mainly be attributed to the increasing PD intensity and the associated thermal stress on the insulating material test samples. The increase in PD intensity with higher frequencies can be verified both, visually (Figure 9) and through measured partial discharge pulses. It could be observed that the number of PD pulses increased significantly for higher frequencies. Also, the maximum PD levels have increased. The temperature measured under HFHV stress via the ground electrode reached up to approximately 90 °C, while no temperature increase was observed under both 50 Hz and MXF-HV stress. As a result of high

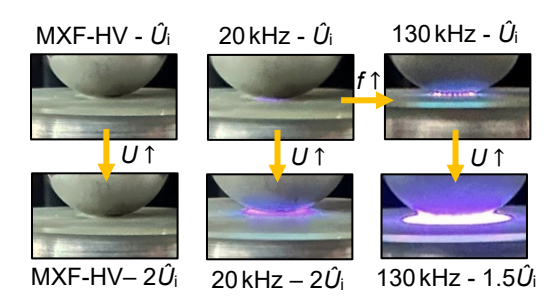


Figure 8: Examples for the optical PD-intensity as a function of voltage and frequency

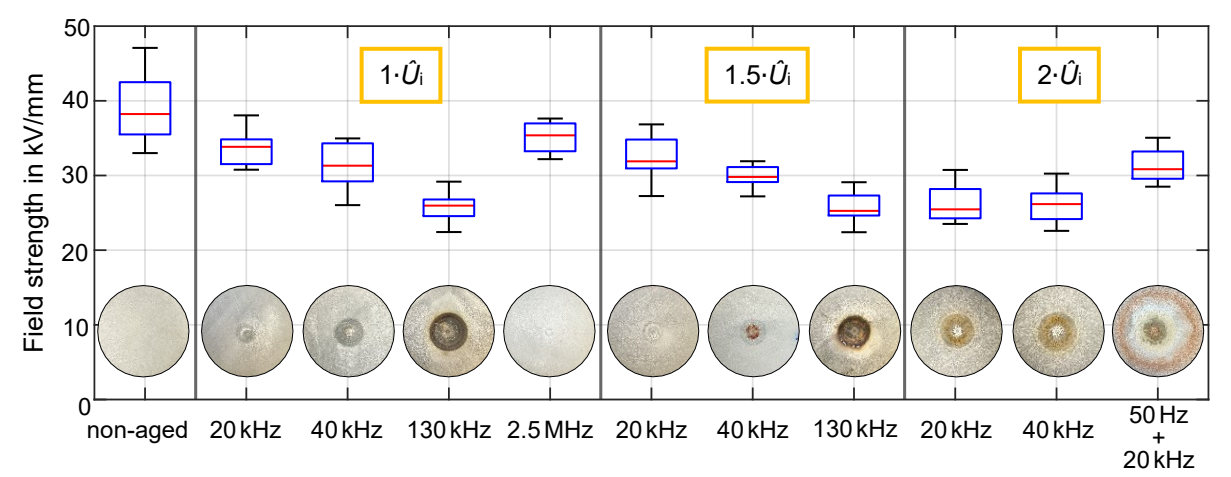


Figure 9: Comparison of breakdown field strengths of non-aged material test samples with material samples aged with the indicated combinations of field strength and frequency

temperatures, chain breaks occur in the molecular structure, along with oxidation, depolarization processes, and the volatilization of low-molecular-weight components [8]. These processes can lead to an increase in conductivity, thus justifying the comparable trend of the loss factor [8]. On the other hand, the surface of the test samples erodes, and additional mechanical stresses arise due to thermal stress, which results in material fatigue.

In case of the HFHV measurement series with 2.5 MHz only unexpectedly minor impacts on both, the dielectric parameters and the breakdown field strength were detected. The reason for this is attributed to the short stress duration.

6. Conclusion

Destructive and non-destructive approaches were employed to investigate the aging behavior of epoxy resin test samples during the presence of partial discharges (surface discharges). As test voltages, 50 Hz, mixed-frequency and several high frequency high voltages, were used. The high frequencies range from 20 kHz to 2.5 MHz. In order to quantify the stress caused by each combination of field strength and frequency to the test samples, the different lifetimes, the changes in dielectric parameters and the changes in breakdown field strength were determined for each aging scenario. All three approaches have shown that high frequency high voltage stress represents a significantly more critical case in terms of PD-aging compared to a 50 Hz stress.

The average lifetime of the test samples was reduced to around 30 seconds in the worst case at 2.5 MHz. For the other HFHV scenarios, the average lifetime was between several minutes and 16 hours. In comparison, no test sample failed during the measurement series with both, power frequency and mixed-frequency within the maximum stress duration of 10 weeks.

Regarding the dielectric parameters a comparable behavior could be observed. In the measurement series with HFHV, PD-aging led to an increase in conductivity and loss factor of up to 200%. In case of the mixed-frequency stress scenarios, on the other hand, an aging behavior comparable to the scenarios with 50 Hz power frequency stress was detected. In these cases, only a slightly increasing trend in conductivity and loss factor could be observed. Regarding the relative permittivity, no significant change could be observed in any of the scenarios. Only for the most critical scenarios a slight increase could be detected.

The breakdown field strength decreased by up to 35% for the HFHV measurement series and up to 18% for the mixed-frequency measurement series. Since no significant decrease could be detected for 50 Hz PD-aging during the given period, in this case aging with mixed-frequencies is considered to be more critical.

For both voltage types, high frequency high voltage and mixed-frequency high voltage, the results can mainly be attributed to an increased PD intensity with increasing frequency. Higher PD levels as well as an increase in the amount of PD pulses could be detected. The associated higher temperatures and thermal stress on the test samples lead to erosion on the materials surface and changes in the material structure.

Literature

- [1] A. Q. Huang, M. L. Crow, et al., "The Future Renewable Electric Energy Delivery and Management (FREEDM) System: The Energy Internet", Proceedings of the IEEE, vol. 99, no. 1, 2011.
 - DOI: 10.1109/JPROC.2010.2081330
- [2] S. K. Rönnberg, M. H. J. Bollen, et al., "On waveform distortion in the frequency range of 2kHz-150kHz-Review and research challenges", Electric Power Systems Research, vol. 150, 2017.
 - DOI: <u>10.1016/j.epsr.2017.04.032.</u>
- [3] G. Longobardi: "GaN for power devices: Benefits, applications, and normally-off technologies", International Semiconductor Conference (CAS), Romania, 2017. DOI: 10.1109/SMICND.2017.8101144
- [4] B. Zhang, M. Ghassemi, Y. Zhang: "Insulation Materials and Systems for Power Electronics Modules: A Review Identifying Challenges and Future Research Needs", IEEE Transactions on Dielectrics and Electrical Insulation Band 28, 2021.
 - DOI: 10.1109/TDEI.2020.009041
- [5] IEC TS 61934-ED3, "Electrical measurement of partial discharges (PD) under short rise time and repetitive voltage impulses", 2023
- [6] IEC 60243-1, "Electric strength of insulating materials Test methods Part 1: Tests at power frequencies.", Edition 3.0, 2013, International Electrotechnical Commission.
- [7] ASTM D149, "Standard Test Method for Dielectric Breakdown Voltage and Dielectric Strength of Solid Electrical Insulating Materials at Commercial Power Frequencies.", 2013.
- [8] Kao, Kwan C, "Dielectric phenomena in solids. With emphasis on physical concepts of electronic processes", Amsterdam, Heidelberg, 2004.

DOI: <u>10.1016/B978-0-12-396561-5.X5010-5</u>